

Philadelphia College of Osteopathic Medicine DigitalCommons@PCOM

PCOM Biomedical Studies Student Scholarship

Student Dissertations, Theses and Papers

2015

The Influence of Matrix Stiffness on Extracellular Matrix Protein Expression in 3D Encapsulated Mammary Fibroblasts

Kathryn Woods

Philadelphia College of Osteopathic Medicine, kathrynwo@pcom.edu

Follow this and additional works at: <http://digitalcommons.pcom.edu/biomed>

 Part of the [Cancer Biology Commons](#), and the [Neoplasms Commons](#)

Recommended Citation

Woods, Kathryn, "The Influence of Matrix Stiffness on Extracellular Matrix Protein Expression in 3D Encapsulated Mammary Fibroblasts" (2015). *PCOM Biomedical Studies Student Scholarship*. Paper 95.

This Thesis is brought to you for free and open access by the Student Dissertations, Theses and Papers at DigitalCommons@PCOM. It has been accepted for inclusion in PCOM Biomedical Studies Student Scholarship by an authorized administrator of DigitalCommons@PCOM. For more information, please contact library@pcom.edu.

Georgia Campus - Philadelphia College of Osteopathic Medicine

The Biomedical Sciences Program

Biomedical Sciences Department

**The Influence of Matrix Stiffness on Extracellular Matrix Protein Expression
in 3D Encapsulated Mammary Fibroblasts**

A Thesis by Kathryn Woods

Advisor: Abigail Hielscher, Ph.D.

Submitted in Partial Fulfillment of the Requirement for the Degree of Master of

Science in Biomedical Sciences June 2015

PCOM Biomedical Sciences Degree Program

Signatory Page for Master's Thesis

We approve the thesis of Kathryn Woods.

Abigail Hielscher, PhD

Assistant Professor of Anatomy

Thesis Advisor

Date of Signature

Richard White, PhD

Professor of Neuroscience Pharmacology & Physiology

Date of Signature

Adwoa D. Aduonum, PhD

Associate Professor of Neuroscience & Physiology

Date of Signature

Brian Matayoshi, PhD

Associate Director, Biomedical Science

Graduate Program

Professor of Physiology

Date of Signature

Abstract

A disease that transcends all races is breast cancer, the second leading cause of death among women with cancer. One factor, which participates in breast tumor progression, is the extracellular matrix (ECM), an acellular, protein-rich entity, which drives several cell processes shown to promote tumorigenesis. Specifically, abnormal expression patterns and cross-linking of matrix fibers induces a more dense tissue structure, which has been reported to drive breast cancer progression. Alterations in ECM expression and crosslinking are in part due to carcinoma-associated fibroblasts (CAFs), activated fibroblasts which deposit copious ECM in the breast tumor environment. The goal of this study is to understand how ECM expression patterns change following culture of human mammary fibroblasts (HMFs) in mechanically tuned 3 dimensional gelatin hydrogels, a culture setup that better mimics the natural breast environment. Since matrix stiffness has been reported to drive the myofibroblast phenotype, it is anticipated that altered ECM expression and deposition patterns will accompany HMF culture in mechanically stiff gelatin hydrogels. To alter the stiffness of the gel, microbial transglutaminase, which cross-links lysine and glutamine residues in the gelatin matrix, will be employed and rheology will be subsequently utilized to determine the bulk mechanical stiffness of cross-linked gels. Three gels with various stiffnesses including compliant, moderate, and stiff will be utilized for encapsulation of HMFs. Viability assays, such as the Live/Dead assay, will be utilized to monitor cell viability over the 7-day culture period. To assess whether matrix stiffness induces unique patterns of matrix expression, we will evaluate ECM protein expression using western blot for the following ECM proteins: tenascin-C, fibronectin, laminin and collagens I, IV. In addition, immunofluorescence will be utilized

to evaluate cellular deposition of ECM proteins in the gelatin hydrogel. Results from these assays will elucidate whether increasing matrix stiffness induces a more pronounced expression level of the aforementioned ECM proteins. Results from these studies may allow for future development of novel therapeutic agents targeted to the myofibroblast within the breast cancer microenvironment.

Table of Contents

Abstract	2
List of Figures	5
List of Abbreviations	6
Acknowledgements	7
Background	9
Hypothesis	16
Specific Aims	16
Methods	18
Results	
mTG Treatment of HMFs in 2D Culture	26
Thermal Stability	28
Gel Stiffness/Rheology	30
Collagenase Digestion of mTG Hydrogels	32
HMF Morphology in mTG Cross-Linked Hydrogels	34
HMF Viability in mTG Cross-Linked Gelatin Hydrogels	37
ECM Protein Expression in Conditioned Media	40
DC Assay for Analysis of Protein Concentration	42
ECM Protein Expression in HMF Protein Lysate	44
Immunofluorescence for ECM Protein Expression	46
Discussion	48
Conclusion	53
References	54

List of Figures

1. 2D HMFs Treated with mTG
2. Thermal Stability of mTG Gelatin
3. Gel Stiffness in Response to mTG
4. Enzymatic Stability of mTG Gelatin
5. 3D Hydrogel HMF Culture System
6. HMF Morphology in mTG Gels
7. HMFs are Viable in mTG Gels
8. ECM Protein Expression from HMFs in mTG Gels –Conditioned Media
9. DC Assay Results
10. ECM Protein Expression from HMFs in mTG Gels – Protein Lysate
11. Immunofluorescence Images

List of Abbreviations

2D – Two-Dimensional

3D – Three-Dimensional

α -SMA – alpha-Smooth Muscle Actin

BME – 2-Mercaptoethanol

BSA – Bovine Serum Albumin

CAFs – Cancer Associated Fibroblasts

Col – Collagen

ECM – Extracellular Matrix

EMT – Epithelial to Mesenchymal Transition

Fn – Fibronectin

HMF – Human Mammary Fibroblasts

mTG – Microbial Transglutaminase

SDS-PAGE – Sodium Dodecyl Sulfate Polyacrylamide Gel Electrophoresis

Acknowledgments

First and foremost, I thank God for providing me the opportunity to complete this program, the focus and fortitude to stay committed, and the intelligence to complete it to the best of my ability. I thank my family, my father, mother, sister, brother, and grandmother as well as many other extended family members, close friends, and church family that have rallied around me in support, encouragement, and love. Their presence has been the backbone that held me up in more difficult times. Continually, I have an immense appreciation and thankfulness for Dr. Abby Hielscher. Her dedication to me from the very beginning is what helped to spark a confidence in me for research that I never knew I had. She has helped in so many ways, not only as an advisor but also as a mentor helping in my transition to my doctoral program, and as a friend in her constant encouragement of me, at every turn. I would also like to give special recognition to Dr. Brian Matayoshi who is simply an advocate for his students. His belief in me has helped to progress me through this program to a successful completion, and I am forever thankful to him for his kind yet thought provoking messages to me, when I needed them most. Just as well, I would like to give special thanks to Dr. Valerie Cadet. She has been another great mentor of mine and has loved and supported me, our many conversations have truly been instrumental in getting me to this point. To Mrs. Linda Williams, I want to acknowledge her love for all of the students, but especially for me. She has been a wonderfully strong presence and such a loving spirit throughout my time at PCOM. I sincerely thank Handong Ma and Yan Wu for their time, advice, and assistance given to me as I learned and grew while working in the laboratory. I also graciously thank Parmjit Jat (University College London) for the human mammary fibroblasts that were donated

for use. Lastly, I am most appreciative of Sharon Gerecht (Johns Hopkins University) for use of the rheometer to measure gel bulk mechanical stiffness.

Introduction

Breast Cancer

Breast cancer is the second leading cause of death among women with cancer (DeSantis, 2011). Approximately 232,670 new cases of invasive breast cancer (IBC) and 40,000 breast cancer deaths are expected to occur among US women in 2014 (Siegel, 2014).

IBC is a general type of breast cancer with a few subtypes detailing the specific location or way in which the cancer metastasizes outside of the breast tissue. Breast cancer commonly arises from abnormal cells, which proliferate within the duct, and is referred to as ductal carcinoma in-situ (DCIS). The difference between IBC and DCIS is that DCIS has not spread from the ducts into the surrounding breast tissue. It progresses from DCIS to invasive and metastatic cancer once the cancer cells breach the basement membrane and intravasate into the blood and lymph vessels (Kalluri, 2006). While many researchers have spent a great deal of time focusing on the cancer cells, recent efforts have focused on the role of the microenvironment in breast tumor progression. The microenvironment is composed of extracellular matrix (ECM), fibroblasts, blood, lymph vessels, nerves, and inflammatory cells which are collectively referred to as the stroma (Kalluri, 2006). One of the major cell structures that make up the connective tissue stroma is fibroblasts. They are non-vascular, non-epithelial, and non-inflammatory cells that are found throughout the connective tissue of the breast (Mangia, 2011). This stroma supports breast homeostasis and helps maintain its structure. When aberrant, the stroma actively participates in breast tumor formation and progression.

Myofibroblasts and Carcinoma-Associated Fibroblasts

One of the major differences observed in the breast tumor microenvironment is the change to the stroma. In the absence of malignancy, the breast tissue contains a small number of fibroblasts and a physiological ECM; whereas, in breast cancer, the stroma becomes reactive (Rønnov-Jessen, 2009). The reactive stroma of breast cancers is usually characterized by a significant loss of myoepithelial cells and basement membrane, in addition to increased number of fibroblasts and myofibroblasts, which deposit a copious ECM matrix, as well as an influx of infiltrating immune cells (Kalluri, 2006; Rønnov-Jessen, 2009). Myofibroblasts are activated fibroblasts characterized by the presence of alpha-smooth muscle actin (α -SMA), which is a component of the actin cytoskeleton, which increases the contractile ability of fibroblasts (Hinz, 2001; Yamashita, 2012). With regard to tissue homeostasis, the myofibroblast participates in wound healing, where it promotes remodeling of the connective tissue following injury (Yamashita, 2012). In cancers, myofibroblasts are referred to as carcinoma-associated fibroblasts (CAFs). CAFs are principally characterized by the expression of α -SMA and vimentin (a protein expressed in invasive cancers, related to high tumor invasion and chemoresistance) and the presence of actin stress fibers (Rønnov-Jessen, 1996; Tsukada, 1987; Gabbiani, 2003; Kalluri, 2006). CAFs promote breast cancer progression by influencing biological processes such as, cell-ECM adhesion, migration and invasion, and epithelial-mesenchymal transition (EMT) (Yu, 2014). For example, Yu et al (2014), cultured several breast cancer cell lines with CAFs or their conditioned media, reporting that these cell lines showed a more aggressive phenotype due to TGF- β 1 signaling from the CAFs (Yu, 2014). Furthermore, the CAFs in this study were shown to induce tumorigenesis

from normal epithelial cells, by inducing EMT (Yu, 2014), a phenomenon that allows cancer cells to initiate the metastatic cascade.

ECM Proteins and Breast Cancer Progression

The ECM is comprised of several proteoglycans and proteins and is thus a component of the non-cellular niche that actively sustains the morphology of tissues within organs (Lu, 2012). Under homeostatic conditions, the ECM participates in embryological development and wound healing (Lu, 2012). A couple important considerations of ECM biology is (1.) its biomechanical properties, which allows a cell to sense external forces generated by the ECM (Paszek et al., 2005; Lopez et al., 2008; Gehler et al., 2009), and (2.) its overall protein constituents contribute to disease (McBeath et al., 2004; Reilly and Engler, 2010). In breast cancer, for example, ECM proteins are aberrantly expressed in the matrix, contributing to increased tissue rigidity (Paszek et al., 2005), vascular morphogenesis (Hielscher et al 2012), and tumor invasion (Provenzano et al 2006, 2008). ECM proteins, which are abnormally expressed in the breast tumor microenvironment or have been shown to participate in breast tumor progression, include tenascin-C (Oskarsson et al, 2011; Hancox et al, 2009), fibronectin (Barkan et al, 2008; Williams et al 2008), laminin (Kim et al, 2012) and collagens I (Provenzano et al, 2006, 2008) and collagen IV (Nakano et al, 1999).

Fibronectin has been shown to be one of the components driving myofibroblast differentiation from normal fibroblasts (Hinz, 2007). It is also involved with cell-cell

and cell-matrix adhesions, cell migration, morphogenesis, differentiation and oncogene transformation (Gould, 1990). Similar to fibronectin, tenascin-C is a glycoprotein, which influences cellular adhesion, migration, morphogenesis and oncogenic alterations (Gould, 1990; Ioachim, 2002). Laminin and collagen-IV are found within the basement membrane of the ECM (Ioachim, 2002). Laminin is reported to regulate cell migration and adhesion and participates in tumor invasion (Nielsen, 1984; Koochekpour, 1995; Ioachim, 2002). Collagen-IV on the other hand, has been reported to control mammary cell proliferation along with cell adhesion and migration (Kim, 1994; Ioachim, 2002).

The hardening of tissue or ‘lump’ in the breast is one of the initial physical signs of malignancy. This dense tissue is comprised of increased ECM protein expression and remodeling in the form of matrix cross-linking (Butcher, 2009 and Sinkus, 2000). The increased stiffness of the ECM has been shown to promote tumor cell growth, survival, and migration (Lo, 2000). Most importantly, matrix stiffness has been shown to facilitate an activated fibroblast phenotype (Peyton et al, 2006, 2008). For example, Peyton et al, (2006) cultured smooth muscle cells atop mechanically tuned poly(ethylene) glycol (PEG) hydrogels functionalized with cell adhesive binding sites. Increased matrix stiffness combined with different cell adhesive sites promoted cell spreading, proliferation and focal adhesions and F-actin fiber formation, properties, which are indicative of an activated phenotype (Peyton, 2006). Further work by Peyton et al, (2008) have implicated the impact of ECM mechanics in 3D for cancer progression. Consequently, it has become commonly accepted that matrix stiffness is a feature of the tumor microenvironment and therefore participates in cancer progression. Thus, cancer progression occurs due to the cell’s tractional forces, which are balanced against the

ECM matrix rigidity allowing cells to migrate and move along the matrix that is able to resist the force (Peyton, 2008). Overall, investigating the role of matrix stiffness on cell responses is an important concept for understanding the role of substrate compliance on tumor progression. In order to investigate the impact of matrix stiffness on cell behavior, a biologically relevant culture setup is necessary.

Three Dimensional Culture

In order to better recapitulate cellular activities *in vitro*, it is important to culture cells in a substrate that mimics their *in-vivo* environment. Science has advanced over the years and has provided the ability to understand these concepts using a natural model of the cellular environment within cell culture, via two-dimensional (2D) and three-dimensional (3D) substrates. 2D cell culture is based on the growth of single cell populations on a flat surface substrate, such as tissue culture polystyrene. However, there are several limitations to the 2D culture substrate (Engler, 2007; Chen, 1997; Singhvi, 1994). Some of these restraints include the confinement of cells to a planar environment that suppresses more complex morphologies (Tibbit, 2009). Also, cells grown on this platform are evidenced to experience minimal resistance to migration from lack of surrounding ECM (Tibbit, 2009). As a result, it is essential for cells to be cultured in an environment which better represents normal cell activities, such as cell-cell and cell-ECM interactions, cell signaling and growth, responses to exogenous factors, and cancer metastasis and tissue organization (Tibbit, 2009). To overcome the limitations of 2D culture, cell growth in 3D environments has been increasingly used (Tibbit, 2009).

Hydrogels (used for 3D cellular culture) are a network of polymer chains principally made up of water, giving the hydrogel a natural tissue-like state useful for cell

culture (Nguyen and West, 2002). Specifically, gelatin hydrogels are desirable for a number of reasons. For example, gelatin is the denatured product of collagen, a ubiquitous protein in the breast microenvironment (Sung, 2014), making it a relevant scaffold for use to mimic the breast tumor microenvironment. Gelatin is also a desirable substrate since it is non-immunogenic, easy to use and can be mechanically modified using enzymatic approaches (Nimni, 1988).

Transglutaminase

The use of a cross-linking agent to tune the mechanical stiffness of hydrogels has become necessary and relevant to cell and tissue culture in biomedical research. Although a number of methods including UV light, glutaraldehyde and formaldehyde may be used to cross-link hydrogels, these agents are toxic to cells (Chen, 2005). As such, enzymatic methods have been adapted to induce cross-linking of hydrogels while minimizing toxicity to cells (Chen, 2005). One enzymatic approach is microbial transglutaminase (mTg) derived from *streptovercillium morabense*. Used widely in the food industry, mTg catalyzes protein polymerization by forming intermolecular and intramolecular lysine-glutamine cross-links in gelatin and collagen gels (Chobert, 1996). The mechanism of action for mTg is to catalyze an acyl-transfer reaction; γ -carboxamide groups of peptide-bound glutamine residues act as the acyl donor, and ϵ -amino groups of lysine residues act as the acyl acceptor to perform the protein polymerization bond (Folk, 1980). Aside from its cross-linking activities, other desirable properties of mTg include its wide range of pH stability, the range for controlled expression at different temperatures, and the cross-linking effect on tensile strength seen in the gels (Chen, 2005). Chen et al (2005) showed that following encapsulation of fibroblasts in mTg cross-linked gels, the

gels supported growth and viability of the cells (Chen, 2005). Additionally, studies by Yung et. Al (2007) exhibited the compliance of mTg cross-linked gelatin as a tissue-engineering scaffold for the growth and encapsulation of HEK 293 human embryonic kidney cells. Overall, these studies demonstrate the utility of mTg cross-linked gels as suitable substrates for growth of cells.

Hypothesis

HMFs cultured in a stiff gel as opposed to a compliant gel will exhibit a greater expression of ECM proteins.

Specific Aims

Specific Aim 1: Evaluate the effect of matrix rigidity on HMF cell viability.

HMFs will be encapsulated in compliant, moderate and stiff gelatin hydrogels. In this analysis, 35,000 HMFs will be co-mixed with 7.5% gelatin containing 20 (compliant), 30 (moderate), or 100 (stiff) $\mu\text{g/ml}$ mTgase. The measured stiffness of the varying mTgase concentrations are as follows: compliant, ~ 300 Pascals; moderate $\sim 1,300$ Pascals; stiff/rigid $\sim 2,000$ Pascals. HMFs encapsulated in mTgase cross-linked gelatin will be incubated at 37°C for 30 minutes to facilitate cross-linking and with then be overlaid with 1ml of complete media. The cell morphology and viability are monitored via the Live/Dead assay over a 7-day culture period, and the proportion of live versus dead cells will be quantified using Image J.

Specific Aim 2: Evaluate the effect of matrix rigidity on ECM protein expression.

Expression of several ECM proteins including fibronectin (Sereini, 1998; Tomasek, 2002) , collagens I (Binai, 2012; Hinz, 2007) and IV (Minz, 2010), tenascin-C (El-Karef, 2007), and laminin (Marangon, 2014) are associated with the myofibroblast phenotype and/or breast cancer progression. Western blot will be utilized to quantify the expression of these proteins in both the conditioned media and in HMFs encapsulated in compliant, moderate and stiff gels at days 1,3,5 and 7. The cells will be isolated for Western blot. First, the gels will be digested with tryPLe, then the remnants will be spun down to obtain the cell pellets. The cells will be incubated in a cell lysis buffer containing a protease

inhibitor cocktail. From here, total protein will be quantified using Bradford, then run on an SDS Page gel. Changes in protein expression will be observed using a LI-COR Odyssey imager.

Specific Aim 3: Evaluate the effect of matrix rigidity on ECM protein deposition in 3D.

Extracellular deposition of aforementioned ECM proteins will be evaluated using a Zeiss-LSM510 confocal microscope. This analysis will elucidate whether HMFs in stiff gels deposit greater quantities of matrix proteins in the gel, an observation, which would link matrix stiffness with ECM deposition in 3D. Gel preparation for imaging will be based off methods reported by Wozniak et al, 2003. Briefly, gels will be cut into 5 equal fragments and will be fixed in 4% paraformaldehyde overnight. Gels will be permeabilized using triton-X prior to staining with primary antibodies followed by staining with fluorescent secondary antibodies. Gel fragments will be mounted using Prolong Anti-Fade Mounting Medium and will be imaged the next day at days 1,3, 5 and 7. Results from this work may be utilized in future analyses to evaluate the organization of ECM proteins in the 3D matrix.

Methods

Microbial Transglutaminase Isolation

A mTg solution was prepared using 2.5g crude mTg in 50mL Buffer A (20mM phosphate buffer & 2mM EDTA buffer, pH 6.0) to make a 5% solution. mTg was isolated using column chromatography. Prior to separation, 2.5ml of Sepharose FF beads were given 5 minutes to settle out of solution. The beads were then washed in 5 column volumes (Column Vol = 2.5mL) of Buffer A. Then they were mixed with the mTg solution and left overnight for incubation at 4°C. Following overnight incubation, the protein solution and bead mixture were loaded on a column, and washed with 4 column volumes of Buffer A. Then 3-5mL of Buffer B (NaCl in 20mM phosphate buffer and 2mM EDTA buffer, at pH 6.0) were added to the bead mixture. Fractions were eluted using varying concentrations of NaCl (0mM, 200mM, 400mM, 600mM, 800mM, and 1000 mM NaCl). After addition of Buffer B, the fraction eluant was separated into 1-5mL aliquots. Protein was purified from the NaCl using 10kDa ultracentrifugal spin columns. Concentrations of protein were determined using the DC assay. This is a method for evaluating the concentration of an unknown protein from a given a set of measured known protein concentrations. Absorbance values were obtained at a wavelength of 750nm using a microplate reader. As a purity assurance method, a coomassie stain was run from purified protein on a 4-20% SDS PAGE gel.

Cell Culture

Human mammary fibroblasts (HMFs), an immortalized fibroblast cell line, was obtained from Dr. Parmjit Jat of the University College London. HMF cells were cultured in

DMEM (Life Technologies, Grand Island, NY) supplemented with 10% vol/vol heat inactivated FBS (Life Technologist). Media was replaced every 2-3 days and cells were passaged after reaching 80-90% confluence using 0.25% trypsin EDTA (Sigma, Allentown, PA). HMFs were maintained at 37°C in a humidified atmosphere containing 5% CO₂.

mTG Treatment of 2D HMFs

To determine whether mTG was toxic to HMFs, HMFs were treated with several concentrations of mTg, ranging from 6.3µg/mL to 500µg/mL. Prior to administering mTg, HMFs were plated in a 24 well plate and allowed to incubate overnight prior. The next day, the cells were treated in triplicate with various concentrations of mTg and were left to incubate overnight. HMF viability was measured using the Almar Blue reagent.

Thermal Stability of mTG Hydrogels

To evaluate the thermal stability of mTg cross-linked gelatin, gelatin was cross-linked with 6.3µg/mL and 500µg/mL mTg at 37°C, then 1mL of 1X PBS was added to each gel. Prior to addition of PBS, the gels were weighed to obtain the initial weight, then incubated in 1mL of PBS at 37°C for one hour where weight was measured at each hour up to five hours total. For each weight measurement, PBS was carefully removed from the gels and then added back to the gels for continued incubation.

Rheology of mTg Hydrogels

Rheology was used to measure the bulk mechanical stiffness of the gel. Gelatin hydrogels were cross-linked with 15µg/mL, 20µg/mL, 30µg/mL, 60µg/mL, 75µg/mL, and

100 μ g/mL mTG and incubated at 37⁰C for 2 hours to overnight in 1X PBS. These experiments were performed in collaboration with Kyung Park, Ph.D. and Sharon Gerecht, Ph.D. (Johns Hopkins University, Baltimore, MD).

3D HMF Encapsulation

In order to culture HMFs in gelatin hydrogels, HMFs were trypsinized as described above and 35,000 viable HMFs were encapsulated in 7.5% (3.75g in 50mL solution) gelatin cross-linked with varying concentrations of mTg (20, 30, and 60 μ g). Cell viability was determined using an automated cell counter (Life Technologies). Gelatin was prepared using 1X PBS and sterilized using a steriflip (50ml sterile centrifuge tube top unit with pore size 0.22 μ m). Prior to HMF encapsulation, the sterile gelatin was pre-warmed for 2-3 hours at 37.4⁰C in a water bath. To encapsulate HMFs in gelatin gels, 35,000 viable HMFs cells were resuspended in 20 μ L of serum-free media (DMEM). To this, 250 μ L of gelatin containing 20, 30, and 60 μ g of mTg was added to the cells and the gel encapsulated cell suspension was added to each of 4-10 wells of a 24-well plate. After plating, a gelation time of 30-45 minutes in a 37⁰C incubator was given to enable crosslinking. Upon polymerization, 1 mL of complete media was added to each gel. The gels were maintained at 37⁰C in a humidified atmosphere containing 5% CO₂ for varying time points over a 7-day incubation period.

Viability Assays

The Live/Dead viability assay was used to quantify the amount of viable HMFs found within the various mTg cross-linked hydrogels. Viable HMFs in 20 and 30 μ g mTg gels were evaluated at days 1, 3, 5, and 7 post-encapsulation. Calcein AM (Life Technologies)

and ethidium bromide (Life Technologies) were used at a concentration of $1\mu\text{M}$ each. Both reagents were mixed with 5ml of sterile 1X PBS and added to cell-encapsulated gels at a volume of $500\mu\text{L}$. The gels were incubated in the dark at room temperature for 45 minutes prior to imaging. The EVOS microscope (Life Technologies) was used for imaging live and dead cells. A 10x objective was used to capture images in the GFP (live), RFP (dead), and phase channels. Three sets of images were taken per well at three non-overlapping locations. Images were analyzed using ImageJ (NIH) software, which enabled quantification of live and dead cells. Here, each image was converted to a binary image produce a black/white image that showed white cells on a black background. After this viable and nonviable were manually counted to notate the number of live cells compared to dead cells.

Collagenase Assay

Collagenase (Sigma) was used to liberate HMFs from gelatin hydrogels. At days 1, 3, 5, or 7 of culture, the gelatin hydrogels were washed 3x each with 1X sterile PBS and incubated for 3 hours in $250\mu\text{l}$ of a 0.5mg/mL concentration of collagenase suspended in DMEM media containing $50\mu\text{L}$ of a 100x protease inhibitor cocktail solution (Sigma). Following incubation the contents were centrifuged at 4500 RPM for 10 minutes at 25°C . The supernatant was decanted and the cell pellet was incubated in $500\mu\text{L}$ of ice cold RIPA Buffer with $5\mu\text{L}$ of a 100x protease inhibitor cocktail for 10 minutes. RIPA Buffer contains 150mM NaCl, 1.0% Triton X, 0.5% Sodium Deoxycholate (SDC), 0.1% SDS, and 50mM Tris pH 8.0. The lysed cell contents were microcentrifuged at $12,000 \times g$ for 10 minutes at 4°C the lysate stored in -80°C .

DC Assay

The DC Assay is used to measure the concentrations of unknown proteins based on a set of known bovine serum albumin (BSA) concentration values. Several concentrations of the BSA stock solution were prepared for the known protein concentration solutions (0mg/mL, 0.1mg/mL, 0.25mg/mL, 0.5mg/mL, 1.0mg/mL, 2.0mg/mL, 4.0mg/mL, 6.0mg/mL, 8.0mg/mL, and 10mg/mL). Each known and unknown concentration was added to a 96-well plate, at 5uL per well, in triplicate. Following this, a volume of 25uL SA mix (1mL Reagent A + 20uL Reagent S) was added to well. Finally, 200uL of Reagent B (used to measure the amount of protein in the sample) was placed in each well. The plate was then incubated in the dark at room temperature for 15 minutes. The absorbances were analyzed at 750nm wavelength using a plate reader and the Gen5 software. The absorbances were then plotted in GraphPad Prism software on a graph to attain the concentration vs. absorbance data. A linear regression was used to obtain the slope and equation of the line, which was $y=mx + b$. Where 'y' is the y-intercept, 'm' is the slope, 'x' is the concentration, and 'b' is the absorbance. Each unknown absorbance concentration was calculated, given the absorbance based on the data from the DC Assay. This allowed for the unknown volume needed for each protein to be used for western blotting.

Western Blot

Western blot is used for protein separation based on differences in the weight of proteins within a sample. Conditioned media from HMF encapsulated hydrogels was collected at days 1, 3, 5 and 7 from 20 μ g, 30 μ g, and 60 μ g mTg cross-linked gels. Protein lysate from

HMF encapsulated hydrogels was collected at days 1, 3, 5 and 7 from 20 μ g and 30 μ g mTg cross-linked gels. For collection of lysate from cell-encapsulated gels, the media was not changed during the incubation period. Protein lysate was collected from mTg gelatin hydrogels as previously described using collagenase. For analyses of conditioned media, a volume of 30 μ L (15 μ L conditioned media and 15 μ L laemelli buffer) was loaded per well into a 4-20% SDS PAGE gel (BioRad). As a control, complete media solution was used (15 μ L of complete media and 15 μ L laemelli buffer). A solution of 5 μ L of LICOR molecular weight marker (LICOR, Lincoln, NE) in 25 μ L laemelli buffer was used for the ladder. For analyses on protein lysate, 25 μ g of protein from HMFs isolated from 20 μ g and 30 μ g mTg gels was added to each well of a 4-20% SDS PAGE gel. Prior to loading, 14.75 μ L laemelli buffer and 0.75 μ L BME were added, with additional RIPA buffer to round out the volume of the sample to 30 μ L total. Then, the protein sample was boiled at 95 $^{\circ}$ C for 5 minutes, at which point each protein sample was loaded into the gel. For both the conditioned media and the protein lysate, the gel was run at 200V for 30 minutes using a 1X SDS buffer solution (100mL 10X SDS buffer and 900mL DI water) for the running buffer. After this, the proteins were transferred to PVDF membranes (Biorad), pre-soaked in 100% ethanol, using a semi-dry blot module (TransBlot system). The transfer buffer that was used consisted of (10mL Tris Buffer, 30mL DI water, 10mL 100% ethanol). Membranes were blocked for at least 3 hours, or overnight in Odyssey Blocking Buffer (LI-COR Biosciences, Lincoln, NE). Following this, there was an overnight incubation at 4 $^{\circ}$ C/constant shaking with the following antibodies: rabbit anti-human collagen I (1:2,000), mouse anti-human collagen IV (1:250), rabbit anti-human laminin (1:400), mouse anti-human tenascin C (1: 150), rabbit anti-human fibronectin

(1:300), and rabbit anti-human GAPDH (1:1,000). Each of the antibodies were made up in Odyssey blocking buffer containing 0.1% tween 20. The next day the membranes were washed three times for fifteen minutes each at constant shaking in washing buffer (100 mL 1X PBS, 1mL Tween-20, 900mL DI water). The blots were then incubated in secondary antibodies, [Goat anti-mouse/rabbit (1:10,000)] for one hour at room temperature. The secondary antibody was also made up in Odyssey blocking buffer, Tween-20, and SDS Buffer. After the secondary step, the membranes were washed three times for fifteen minutes each in washing buffer, and then imaged for presence of ECM proteins. The Odyssey CLx (LI-COR) was used for imaging the blots. The 700 channel was used to observe protein bands.

Immunofluorescence Imaging

Immunofluorescence imaging was used to visualize the expression of certain ECM proteins, such as fibronectin and collagen I, in HMF encapsulated hydrogels. 3D hydrogels were removed from culture at respective experimental time points (day 1, 3, 5, and 7), and 3.7% formaldehyde fixative was added to each gel for an overnight incubation at 4⁰C. Then, 0.2% triton-X was added for a 10-20 minute incubation at room temperature. Afterward, 1% donkey serum (blocking step) was added to the hydrogels for overnight incubation at 4⁰C. The gels were then washed 3 times in 1X PBS for 5 minutes each. Next the gels were incubated at 4⁰C overnight in a 1:50 dilution of mouse anti-human fibronectin. The gels were then washed 3 times in 1X PBS for 5 minutes each. Next, the gels were incubated for one hour at room temperature with a 1:100 dilution of phalloidin-488 (Life Technologies) and a 1:100 dilution of anti-mouse Alexa Fluor-568 (Life Technologies). The secondary dilutions were made in 1% donkey serum and

incubations were performed in the dark. The gels were washed again 3 times in 1X PBS for 5 minutes each. Afterward, the gels were incubated in a 1:1000 dilution of DAPI stain for 10 minutes in the dark. The wells were washed 3 times in 1X PBS for 5 minutes each. Following this, the wells were imaged at 10X and 40X magnification with GFP, RFP, DAPI, and phase channels, using the EVOS microscope.

Statistical Analyses

GraphPad Prism software was used for various statistical analyses. It was used to determine the concentration vs. absorption, when analyzing the data from the DC assays. This information ultimately was used to determine the concentrations of the unknown protein samples in the mTg eluant and in the protein lysate from HMFs encapsulated in mTg gels.

GraphPad and Microsoft Excel were also used for determining significance from viability data. Here, a student's t-test was performed by comparing the viability data (% live vs. % dead) for each experimental time point (days 1, 3, 5, and 7) in each gel condition. Anova was also used for multiple data set comparisons in the 2D mTG treatment. Data were reported using a bar graph and the standard deviation. The values of significance were * $p \leq 0.05$, ** $p \leq 0.01$.

Results

mTg Treatment of HMFs in 2D Culture

Since mTg was necessary for cross-linking the 3D hydrogels, it was necessary to first determine whether the enzyme was toxic to HMFs. As a result, the concentration range for the maximum non-toxic amount of mTg that still maintained HMFs viability was determined. The HMFs were treated with various mTg concentrations (6.3 $\mu\text{g}/\text{mL}$ – 500 $\mu\text{g}/\text{mL}$) in a 2D tissue culture polystyrene plate. HMF viability was measured using Almar blue. After treatment, the percent cell viability was measured, and it was determined that HMFs were viable at most mTg concentrations tested. It was found that the HMFs exhibited viabilities ranging from 80% to 105%, where 75-80% viability was considered acceptable (Figure 1). This data was used to help establish the concentration of mTg used for making compliant and stiff gels.

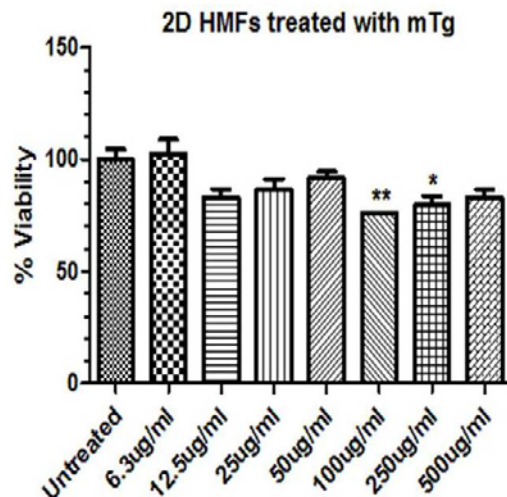
Figure 1

Figure 1: 2D HMFs Treated with mTg. HMFs were treated with varying concentrations of mTg, ranging from 6.3 $\mu\text{g}/\text{mL}$ to 500 $\mu\text{g}/\text{mL}$ in order to determine whether mTg was toxic to the cells. By adding varying mTg concentrations to HMFs grown in 2D polystyrene flasks, the viability was measured and the % viability was analyzed in the graph above. There was significant difference seen in comparing control to 100 $\mu\text{g}/\text{mL}$ and 250 $\mu\text{g}/\text{mL}$, showing a greater compared decrease in viability than the other mTG concentrations. Viability was generally high for each of the tested concentrations with viability of 75-80% or above being acceptable. * $p \leq 0.05$, ** $p \leq 0.01$.

Thermal Stability

After determining that mTg was relatively non-toxic to HMFs, the thermal stability of mTg cross-linked gels was measured. This was necessary as gel encapsulated HMFs were to be maintained in an incubator at 37°C. However, if the gels could not maintain a solid state at higher temperatures, the hydrogels would not be an optimal culture method for the HMFs. As 37°C is the storage temperature for cell cultures, the 37°C incubator was an adequate method to determine the hydrogel's stability. After crosslinking the gels (without HMFs) with 6.3µg/mL and 500µg/mL of mTg, 1mL of 1X PBS was added and the gels were placed in an incubator at 37°C where the weight of the gel was measured following removal of the PBS each hour up to 5 hours. The lowest and highest mTG concentrations were used in order to delineate their varied affect on viability. Incubating the gels in 1X PBS mimicked the culture environment of the hydrogels encapsulated with HMFs. Therefore, any loss of gel weight would signify decreased stability. The weight of the 6.3µg mTg gels somewhat increased in weight over a 5-hour period of time, indicating that this concentration of mTg yields a stable gel, which was found to swell over time (Figure 2). At 500µg mTg, the gels showed a slight decrease in weight throughout the 5 hour time frame (Figure 2).

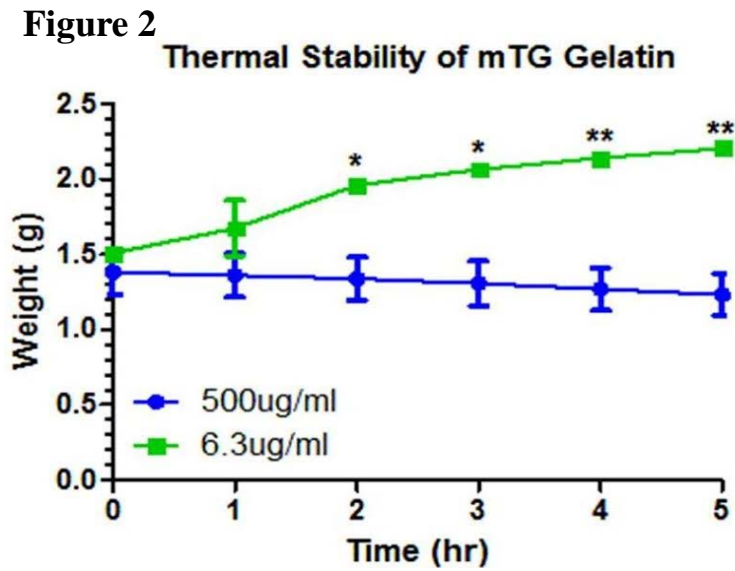


Figure 2: Thermal Stability of mTg Gelatin Hydrogels. Gels were cross-linked with the lowest (6.3µg) and the highest (500µg) tested concentrations of mTg in order to test the thermal stability of the gels. The gels were incubated at 37°C in 1X PBS for 5 hours, where the gel weight was taken at each hour for analyses of stability. PBS was removed prior to weighing. Gels at the lowest mTg concentration swelled over time, while the gels in the highest mTg concentration had slight decrease in weight throughout the incubation period. Significant difference shown by * $p \leq 0.05$, ** $p \leq 0.01$.

Gel Stiffness/Rheology

In order to measure the bulk mechanical stiffness of mTg cross-linked gelatin hydrogels, rheology was used. This procedure allowed for the analysis of stress/strain of the gelatin hydrogels cross-linked with various mTg concentrations. ‘Stress/Strain’ is the degree of compression of biomaterial when a given force applied to it (Battista, 2005). Though colleagues at Johns Hopkins completed the process, the results were utilized for creating hydrogels designed to represent compliant and stiff substrates. The corresponding mechanical stiffness (shown in Pascals) for each of the mTg concentrations tested is listed in in Table 1. The data illustrate that with increasing mTg concentrations, higher mechanical stiffnesses were obtained. While 15 μ g of mTg yielded the most compliant gel, use of this concentration resulted in longer gelation times, which would likely result in death to the encapsulated HMFs. The highest concentrations tested (75 and 100 μ g) of mTg created environments that were exceedingly stiff and were not supportive to cell growth (data provided by Catlyn Thigpen, 2015). As previously mentioned, 60 μ g was also considered for the mTg concentration for mechanically-tuned stiffness. However, due to a lower proliferation shown in 60 μ g compared to 30 μ g, it was not included as being the stiffest hydrogel (from proliferation data from Catlyn Thigpen). Thus, concentrations of 20 and 30 μ g of mTg were utilized for generation of 3D hydrogels representing compliant and stiff scaffolds, respectively.

Table 1

mTg	G' Pascals
15 μ g	100
20 μ g	300
30 μ g	1200
60 μ g	1300
75 μ g	1800
100 μ g	1900

Table 1: Gel Mechanical Stiffness in Response to mTg. Bulk mechanical stiffness of the hydrogels was taken by obtaining rheology measurements. Hydrogels were treated with various concentrations of mTg and were incubated at 37⁰C overnight in 1X PBS to mimic conditions of cell culture. Pascals, (N/m²), was obtained from the stress/strain of the mTg gels.

Collagenase Digestion of mTg Hydrogels

In order to complete several of the downstream studies on the effects of gel matrix stiffness on HMF ECM expression, the HMFs needed to be liberated from the hydrogels. Collagenase was used for this process with varying collagenase concentrations used to determine the optimum concentration and least amount of time needed to dissolve the gel. This was important, as enzyme left too long could damage or kill the HMFs in the gel. Using three different concentrations of collagenase (0.1mg/mL, 0.25mg/mL, and 0.5mg/mL), it was determined that a 3-hour incubation in 0.5mg/mL of collagenase was the most effective concentration to digest the gels and liberate the HMFs encapsulated in 30 μ g mTg gels (Figure 3). It was decided to test collagenase using the 30 μ g gel, because it was the most rigid gel, so the results would be most optimal for any gel type. To prevent loss of protein during the incubation process, 50 μ L of a protease inhibitor cocktail solution was added to the suspension. Each of the trials were completed in triplicate for validity of results.

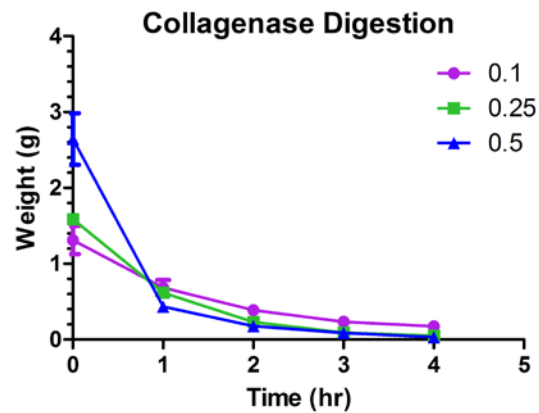
Figure 3

Figure 3: Collagenase Digestion of mTg Gelatin Hydrogels. HMFs were encapsulated in 30 μ g hydrogels and collagenase added to breakdown the gels, liberating the cells. The collagenase enzyme concentrations used were 0.1mg/mL, 0.25mg/mL, and 0.5mg/mL. It was observed that at 3 hours the 0.5mg/mL concentration had more completely broken down the gels. Each trial was completed in triplicate.

HMF Morphology in mTg Cross-Linked Hydrogels

HMFs were encapsulated in mTg cross-linked gelatin hydrogels and observed over the culture period, in order to determine the effects of gel stiffness on HMF cell morphology. A schematic of the culture setup and downstream analyses are shown in Figure 4. In order to visually assess HMFs throughout the experimental period, the change in cell morphology was observed. Following 1 day of encapsulation in 20 μ g (compliant) and 30 μ g (stiff) mTg cross-linked hydrogels, HMFs exhibit a rounded and spherical shape (Figure 5). As the HMFs began to adhere to the surrounding environment, they formed protrusions. These protrusions were observed at days 3 and 5 of culture in the compliant and stiff gels (Figure 5). At day 7, HMFs in the compliant and stiff gels were more pronounced than at earlier time points. This is evidenced by a greater amount of cells seen throughout the wells for both compliant and stiff gels (Figure 5).

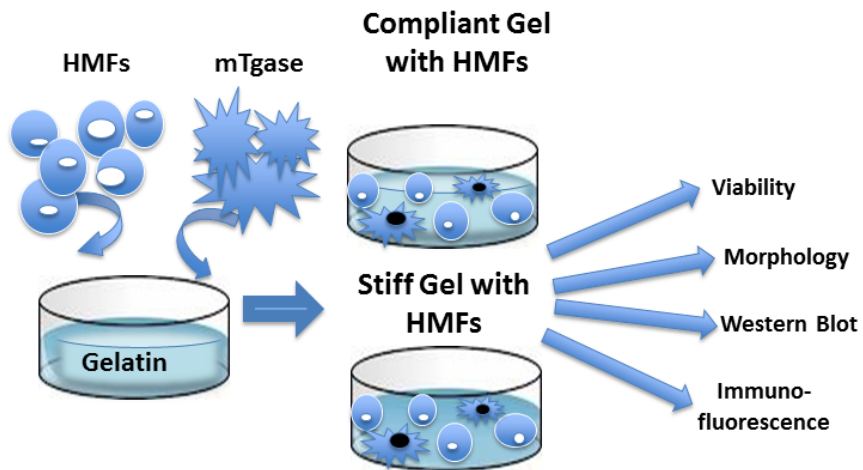
Figure 4

Figure 4: 3D Hydrogel HMF Culture System. HMFs were encapsulated in 7.5% gelatin hydrogels, cross-linked with 20µg (compliant) and 30µg (stiff) of mTg. This culture approach is necessary to assess how mechanical stiffness, achieved using different concentrations of mTg, affected the behavior of HMFs. This schematic details the way that HMFs were encapsulated in mTg gelatin hydrogels to create a 3D scaffold. This culture method served as the basis for all downstream experiments, such as viability, morphology, western blot, and immunofluorescence.

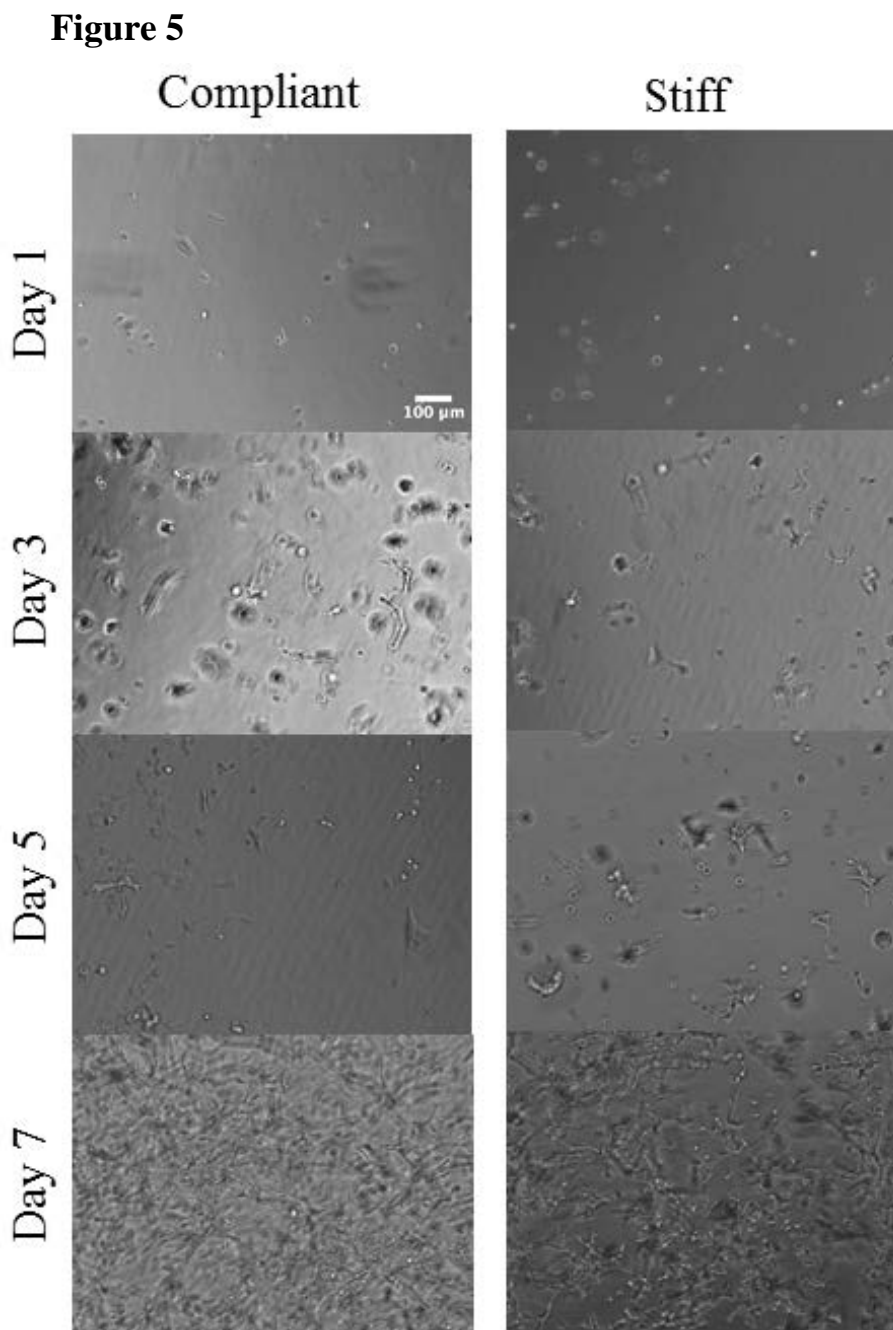


Figure 5: HMF Morphology in mTg Gelatin Hydrogels. Changes in the morphology of HMFs encapsulated in gelatin cross-linked with 20 μ g mTG (compliant) and 30 μ g mTg (stiff) were observed over the 7-day culture period. At day 1 it is seen that the cells are rounded and have similar morphologies. Day 3 shows that the compliant gel has a few more cells present, but in both data sets compliant and stiff cells show some degree of cell spreading. HMFs in Day 5 show that cells have more protrusions but the morphologies are still similar between compliant and sti gels. There are major differences seen at day 7, where cells in the stiff gel are more numerous compared to the cells of the day 7 compliant gel. Images were taken at 10X magnification using the phase channel of the EVOS microscope.

HMF Viability in mTg Cross-Linked Gelatin Hydrogels

Another key component of optimizing the 3D culture system is to ensure that HMFs are viable within the compliant and stiff hydrogels throughout the designated culture period. It was important to assess the cells' viability in order to later measure cell responses within the gel. The denoted period was selected to be 7 days, with the viability assays conducted at days 1, 3, 5, and 7. HMF viability was measured using the Live/Dead assay and imaged using the EVOS microscope with Calcein (live cells) shown via the GFP channel, and ethidium bromide (dead cells) observed via the RFP channel (Figure 6A). The HMFs were then analyzed using ImageJ software for quantifying the number of live and dead cells. Manual counting of binary images from live and dead cells was performed to analyze viability (per day, in either compliant or stiff gels). The compliant gels ranged in viability as follows: Day 1 (25.8%-74.2%), Day 3 (20.4%-79.6%), Day 5 (8.2%-91.8%), and Day 7 (13.7%-86.3%). Comparably, the stiff gels percent viability ranged from, Day 1 (8%-92%), Day 3 (10.1%-88.9%), Day 5 (17.2%-82.8%), and Day 7 (2.7%-97.3%). It was found overall that HMFs are viable throughout the culture period in compliant and stiff mTg cross-linked gels (Figure 6B).

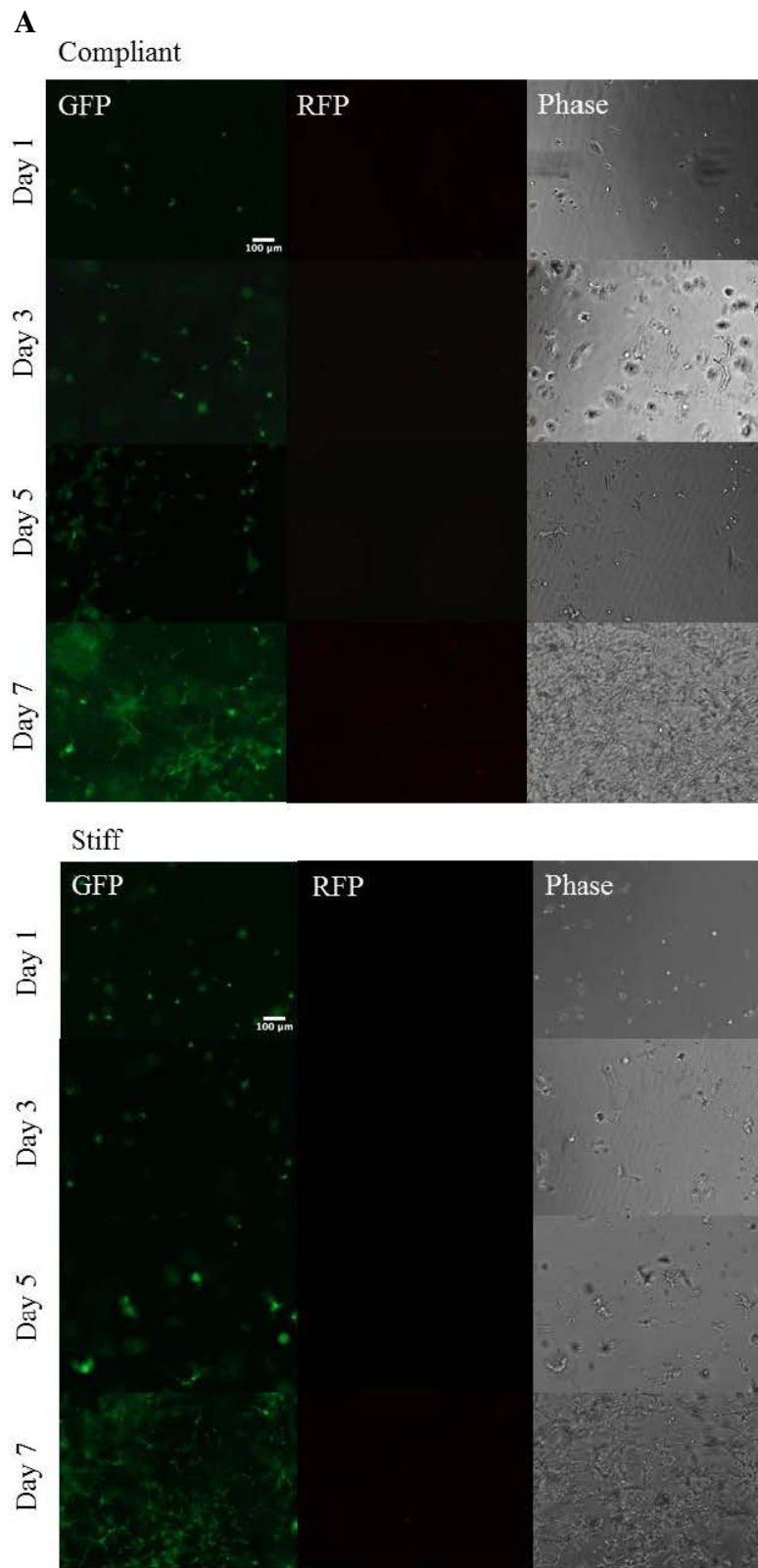
Figure 6

Figure 6: HMF Viability in mTg Gelatin Hydrogels. (A) These images show representative results from the Live/Dead Assay. The GFP channel shows (green) live cells, stained with Calcein. The RFP channel shows (red) dead cells, stained with EtBr. The phase channel shows the cell morphology.

B

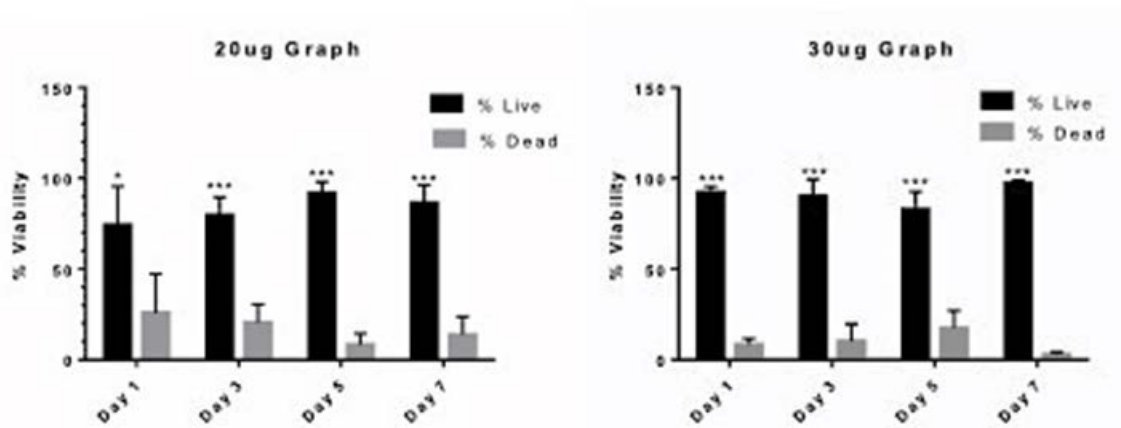


Figure 6: HMF Viability in mTg Gelatin Hydrogels. (B) This data shows that HMFs are viable when encapsulated in mTg gelatin hydrogels in both compliant and stiff mTg concentrations.

ECM Protein Expression in Conditioned Media

The initial method for measuring changes in the expression of ECM proteins was to evaluate ECM protein expression in conditioned media from gel encapsulated HMFs. First, protein in conditioned media from HMFs encapsulated in compliant and stiff hydrogels at days 1, 3, 5, or 7 was collected and separated using 2D SDS PAGE electrophoresis. Then the blots were analyzed for differences in the expression of collagen I, collagen IV, fibronectin, and laminin. Collagen I expression was observed in the compliant gels, but its expression decreased from Day 1 to Day 7 (Figure 7). However, collagen I in the stiff gels had very high expression with Day 3 being the most pronounced (Figure 7). Fibronectin had an overall low expression level for both gel conditions. For the compliant gels, there was some expression, with an overall increase from day 3 through 7, but the stiff gels showed barely any fibronectin (Figure 7). Though the intention was to test the conditioned media for presence of several ECM proteins, after observing little expression of collagen I and fibronectin, it was decided to evaluate ECM expression in cell lysate as opposed to conditioned media.

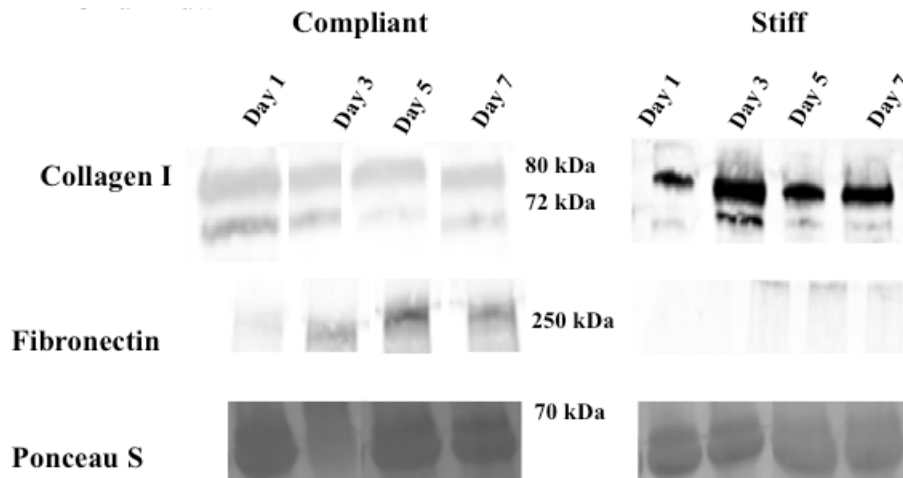
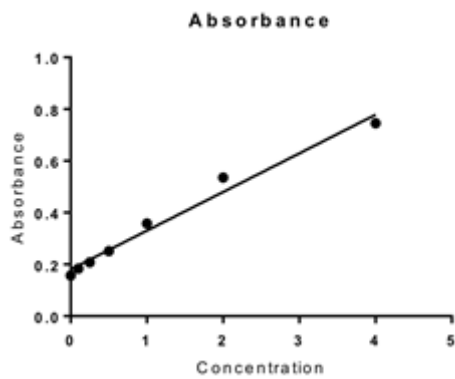
Figure 7

Figure 7: ECM Protein Expression in Conditioned Media. Overall, conditioned media did not express a large amount of ECM proteins. Collagen I had the highest expression in compliant gels expression at day 1. In the stiff gels, collagen I expression was higher than that of compliant gels for all times points. Examining expression in the stiff gels, it was especially high at day 3. Fibronectin had minimal expression overall. Some fibronectin expression was detected in the compliant gels and barely any in the stiff gels. Ponceau S stain was completed as a loading control. The overall purpose of this test was as an initial indicator of ECM protein presence shown in the 3D encapsulated HMFs.

DC Assay for Analyses of Protein Concentration

The DC assay was used to ascertain the concentration of unknown proteins, given the concentration and absorbance of a set of known proteins, based upon varying BSA concentrations. The following data was used specifically to determine the protein concentration and resulting volume to be used for western blot analyses of HMFs encapsulated in 20 μ g and 30 μ g mTG gels (Figure 8). After obtaining the known concentration and absorbance values of the BSA standards, the unknown protein values were determined. This was done by calculating the concentration of each unknown protein, based on the given absorbance values from the known BSA controls.

Figure 8 20ug DC Assay

30ug DC Assay

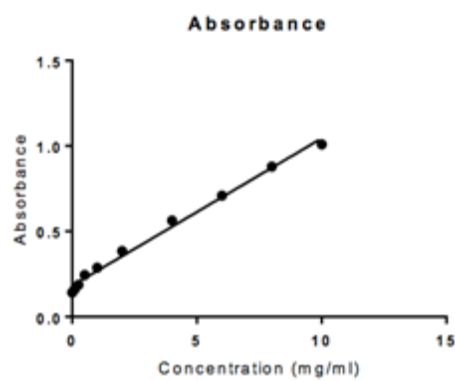


Figure 8. DC Assay of HMF Protein Lysate from Compliant and Stiff Gels. These graphs of known BSA concentrations were obtained by plotting the absorbance readings of BSA known proteins. This data was used to determine the unknown protein concentrations of HMFs encapsulated in compliant and stiff gels. This information was used to further dictate the volume of protein from HMFs in the tested gel conditions to be added to a 2D SDS PAGE Electrophoresis gel for analysis of ECM protein expression.

ECM Protein Expression in HMF Protein Lysate

After testing the conditioned media from the compliant and stiff gels, there was not much ECM protein expression observed except for fibronectin and collagen I. To evaluate ECM protein expression in the cell lysate, the HMFs were liberated via the collagenase assay as described on page 23. Using 2D PAGE electrophoresis and Western blot, protein lysate from compliant and stiff gels at days 1, 3, 5, and 7 were analyzed for the presence of fibronectin, collagen I, collagen IV, laminin, and tenascin-C. Within the compliant gel, the most highly expressed proteins were collagen I, collagen IV, and fibronectin. In comparison to compliant gels, HMFs in stiff gels had a greater level of expression of collagen I between days 1 through 5, with a slight decrease at day 7 (Figure 9). Collagen IV expression was greatest for HMFs in the compliant gel at day 1, and then for HMFs in the stiff gel at days 3, 5, and 7 (Figure 9). Fibronectin expression was greater for HMFs in the compliant gels at all times points tested with the exception of day 7 (Figure 9). Laminin was not detectable in HMFs encapsulated in both the compliant and stiff gels (Figure 10). Tenascin-C had very little expression in HMFs in both gels (Figure 9). GAPDH was the loading control for accuracy of measurements.

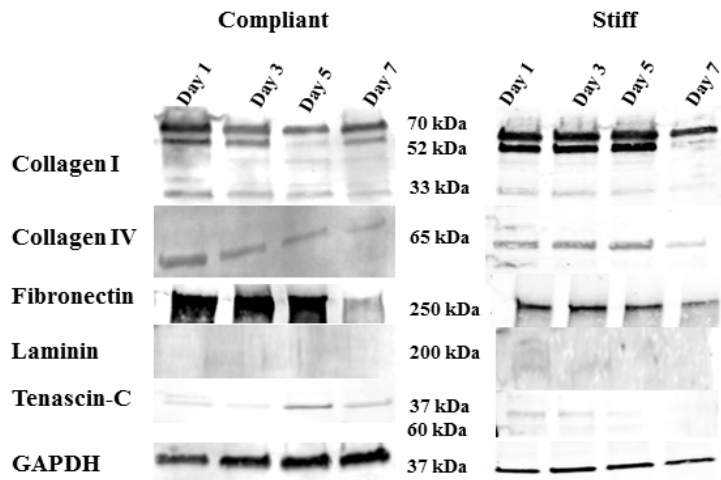
Figure 9

Figure 9: ECM Protein Expression in HMF Protein Lysate. The bands shown detail the ECM protein expression of HMFs encapsulated in compliant and stiff gels. For compliant gels, fibronectin has the highest level of expression. For the stiff gels, collagen I and collagen IV have highest levels of expression. Tenascin-C was evidence at days 5 and 7 in the compliant gels and at day 1 in the stiff gels. Laminin was undetected in both gel conditions. GAPDH was used as the loading control. The images are representative of all data gathered. Each ECM protein test was repeated in triplicate.

Immunofluorescence for ECM Protein Expression

In an attempt to visualize the ECM proteins expressed and/or deposited within the 3D hydrogels, immunofluorescence imaging was employed. Based upon results of ECM protein expression observed from 3D encapsulated HMFs, fibronectin was selected for these analyses as it was highly expressed. To image these proteins, the entire gel was fixed and stained with rabbit anti-human fibronectin primary antibody, along with anti-rabbit Alexa Fluor 546 secondary stain and phalloidin 488, which binds actin filaments. Then DAPI was used to stain the nuclei of the cells. The resulting fibronectin stain was inconclusive; however the phalloidin and DAPI stains were both highly visible. (Figure 10) As this technique did not work, the gel was sectioned down to a more manageable staining size. The gel fragments were stained with rabbit anti-human fibronectin primary antibody, along with anti-rabbit Alexa Fluor 546 secondary stain and phalloidin 488. Results showed that the typical morphology of the HMFs was altered, an observation that may potentially be a result of disruptions in the integrity of the gel once it was pulled out of the well plate (Figure 10). Imaging of the gel fragments revealed a very faint presence of fibronectin staining, though phalloidin and DAPI were robustly shown (Figure 10). Last, the gel was plated into a smaller 96-well plate instead of a 24-well plate since the surface area needed for gel polymerization was decreased. However, no fibronectin staining was observed when imaging (Figure 10). Overall, the methods used for immunofluorescence staining of ECM proteins were not successful. In order to identify fibronectin as well as other ECM proteins, alternate techniques would need to be employed.

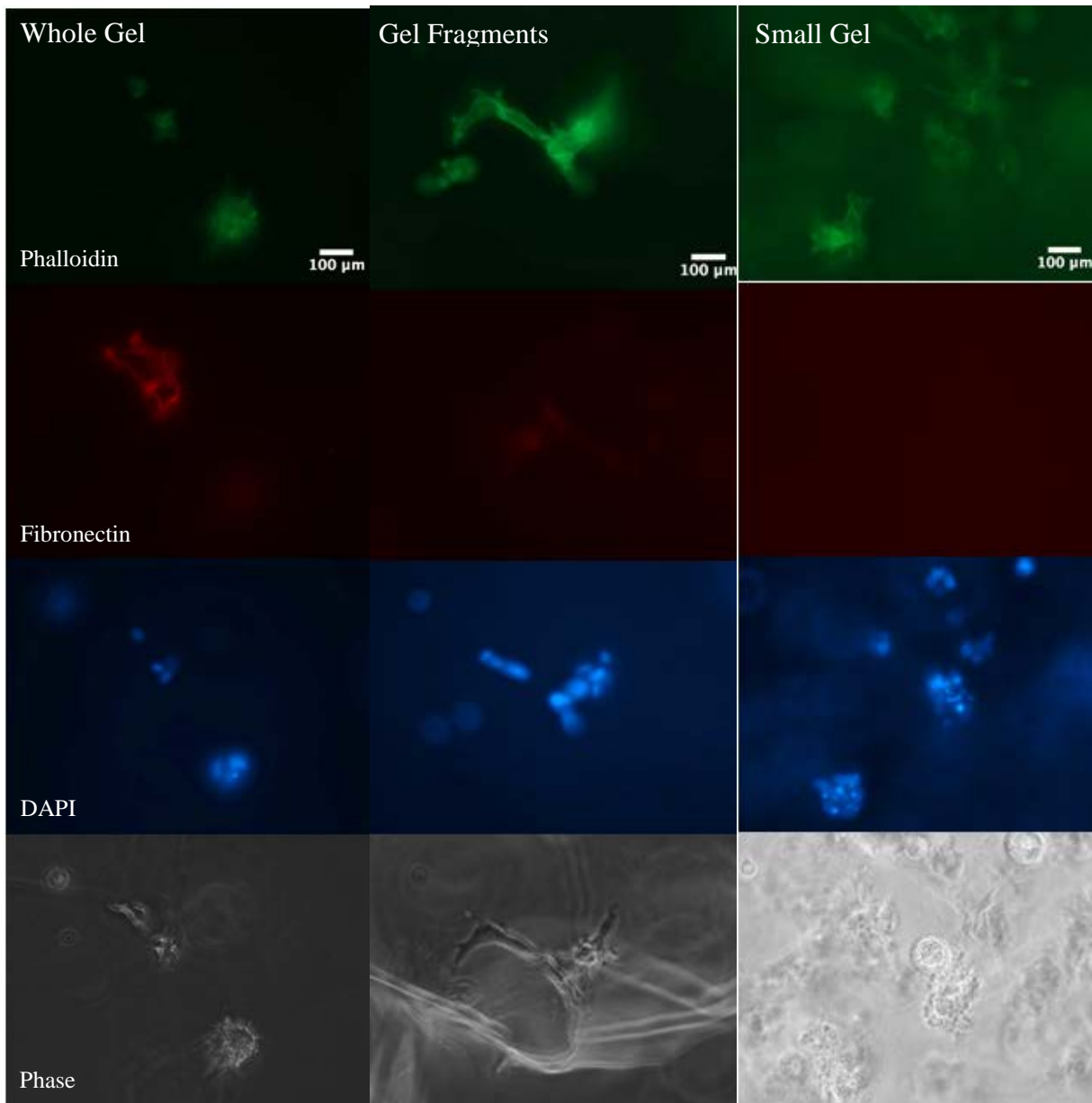
Figure 10

Figure 10. ECM Protein Expression in 3D HMFs. HMFs were analyzed using fluorescence microscopy for their expression of fibronectin. These images illustrate: **(A)** staining in a full gel image. **(B)** staining in a gel that was sectioned. **(C)** staining in a smaller gel surface area, from a 24-well to 96-well plate. Fibronectin was not detectable in any of the stained conditions. The low amount of fibronectin staining is possibly due to lack of adequate methods for visualizing particles within the gel. Also, it is possible that the environment is changing therefore not allowing the ECM proteins to exhibit their true effects from the surrounding stiff environment.

Discussion

Stiffness in breast cancer is a key sign for the initiation of tumor progression. By understanding the effect of the extracellular matrix and fibroblasts, components of the tumor microenvironment, it is possible to gain a clearer sense of the effects these proteins and cells have on tissue stiffness and the production of a more tumor-like environment in the breast tissue. The purpose of this project was to determine the effect that stiffness has on fibroblast cells within a breast tumor-like environment. In order to mimic the tumor environment, a 3D cell culture system was created where hydrogels were mechanically tuned using mTg. The overall hypothesis that HMFs in stiff gels would exhibit enhanced ECM protein expression compared to HMFs in compliant gels was not completely shown throughout this work.

There were several parameters to be optimized prior to completing the encapsulation of HMFs in gelatin gels. Initially, it was determined that mTg was non-toxic to the HMFs grown in 2D tissue culture plastic dishes. This was important because the mTg would be used as the crosslinking agent for the 3D scaffold that would house the HMFs. If the mTg were toxic to HMFs, this would pose an issue for creating the mechanically tuned hydrogels. In similar work, Ito et. al (2003) showed that transglutaminase crosslinking of gelatin promoted fibroblast survival and proliferation. These results allowed for the use of mTg to be tested for its ability to effectively cross-link the gelatin.

Microbial transglutaminase has been shown to be an ideal crosslinking agent for creating hydrogels from thermally cooled gelatin (Yung, 2007). Here, gelatin hydrogels

were cross-linked with mTg and examined for changes in thermal stability. These tests were important in that the hydrogels would not maintain their solid, polymerized state in higher temperatures if mTg did not effectively cross-link the gelatin network. At 500 $\mu\text{g}/\text{mL}$, the highest mTg concentration, the gel weight decreased slightly. At 6.3 $\mu\text{g}/\text{mL}$, the lowest mTg concentration, the gels exhibited some swelling, but overall both concentrations yielded thermally stable gels. Thus, these results show that using too little mTg would cause the hydrogel to retain liquids, potentially a result of the limited number of cross-links in the matrix. Contrary, the greater amount of mTg in hydrogels showed a slight decrease in the gel weight, meaning that too much mTg may reduce liquid retention as a result of increased number of cross-links in the hydrogels.

Since the gels were thermally stable, these data allowed for subsequent measurements of the bulk mechanical stiffness, which was performed using rheology.

Pelham and Wang, for example, observed gels of varying stiffnesses (Wang, 1997).

Rheological measurements of hydrogels cross-linked with different concentrations of mTg would enable the development of mechanically tuned hydrogels, which would serve as a basis for determining the influence of matrix stiffness on fibroblast responses.

Therefore, the measure of stress/strain was recorded, where increased mTg concentrations yielded higher bulk mechanical stiffnesses, measured in Pascals. From these results, several concentrations were selected to serve as compliant 20 $\mu\text{g}/\text{mL}$ mTg (300 Pascals), moderately stiff, 30 $\mu\text{g}/\text{mL}$ mTg (1200 Pascals) and stiff, 60 $\mu\text{g}/\text{mL}$ mTg (1300 Pascals) hydrogels. Through work completed by Catlyn Thigpen, it was shown that the 60 $\mu\text{g}/\text{mL}$ mTg show yielded HMF proliferation that was significantly decreased in comparison to the compliant (20 $\mu\text{g}/\text{mL}$) and moderately stiff (30 $\mu\text{g}/\text{mL}$) gels.

To determine whether higher concentration of mTg yielded different responses, 75 $\mu\text{g}/\text{mL}$ (1800 Pascals) and 100 $\mu\text{g}/\text{mL}$ mTg gels (1900 Pascals) were also tested on the cells. Results from these studies showed non-viable cells over a 7-day culture period; the environment was too stiff for the cells to remain alive for experimental procedures (procedures performed by Catlyn Thigpen). This information allowed for the compliant and stiff gels to be determined as 20 $\mu\text{g}/\text{mL}$ and 30 $\mu\text{g}/\text{mL}$ of mTG, respectively. Enzymatic stability was next evaluated. Collagenase was used to digest the gelatin in order to free the HMFs for further experiments. This experiment was used to gain the most efficient concentration of enzyme for the quickest digestion time. Three different concentrations were evaluated: 0.1mg/mL, 0.25mg/mL, and 0.5mg/mL. The 0.5mg/mL concentration had the shortest time for digesting gelatin cross-linked with 30 $\mu\text{g}/\text{mL}$ mTg. This permitted a better understanding of the concentration of collagenase needed for breakdown of the gelatin and thus, liberation of the encapsulated HMFs.

Following analysis of gel physical properties following cross-linkage with mTg, HMFs were next encapsulated in 3D gelatin hydrogels cross-linked with concentrations of mTg yielding (20 $\mu\text{g}/\text{mL}$) compliant and (30 $\mu\text{g}/\text{mL}$) stiff gels. A cell culture system was created, whereby HMFs were in suspension with serum free DMEM, 20 $\mu\text{g}/\text{mL}$ or 30 $\mu\text{g}/\text{mL}$ mTg, and gelatin. After gelation time, media was added to each gel for its culture period. This system served as the basis for the experimental work. After encapsulating HMFs in mTg cross-linked gels, HMF viability over the 7-day culture period was measured. Previous work by Bott et., al showed that fibroblasts encapsulated in a gelatin hydrogel covalently cross-linked, showed positive proliferation and viability outcomes (Bott, 2010). Similarly, it was shown that gelatin hydrogels cross-linked with

20 μ g/mL (compliant) and 30 μ g/mL (stiff) mTg support HMF viability and growth during the 7-day culture period. Specifically, the percent viability was measured in HMFs encapsulated in each of the gel conditions. Results showed that in both the compliant and stiff gels, the percent viable cells were significantly greater than the percent dead cells during the entire 7-day culture period. This shows that the 3D culture method for growing encapsulated HMFs is an optimal method of 3D cell culture.

To determine whether ECM proteins are upregulated in HMFs exposed to a stiff as opposed to a compliant environment, conditioned media and cell lysate were examined. ECM protein expression patterns varied between HMFs encapsulated in compliant compared to stiff gels. Fibronectin had the highest expression overall in HMFs encapsulated in the compliant gels. This may be potentially explained by fibronectin's action in breast tumor initiation, where it is possible the tumor itself may not be very stiff yet. For example, others have shown higher fibronectin expression in the beginning stages of breast cancer (Tomasek, 2002). Collagen I, a protein associated with breast tumor progression (Hinz, 2007), was found to be more highly expressed in HMFs encapsulated in stiff gels as opposed to compliant gels. Collagen I expression is highly correlated with stiffness in the breast tumor environment. Tenascin-C (Midwood, 2009) and collagen IV (Minz, 2010) are also highly expressed in breast cancer but in both compliant and stiff gels the expression level in HMFs was minimal for each gel condition. Laminin is a basement membrane protein of the ECM (Marangon, 2014). It is unclear why there was no laminin shown in the compliant or stiff gels. It is possible that due to the lack of basement membrane within the hydrogel, laminin was not seen in either the compliant or stiff gels.

Overall, the presence of the ECM proteins was observed, however not as much as expected in the stiff gels more specifically. To determine whether there was as strong a presence of fibronectin (as seen in the compliant gels), immunofluorescence imaging was completed. Work from researchers like Paguirigan et. al (2006) showed the low autofluorescence of the structural components in the hydrogel would indicate that cellular proteins should be observed in 3D hydrogels using immunofluorescence. In a continued effort to observe ECM protein expression within the encapsulated HMFs in both compliant and stiff gels, immunofluorescence staining and imaging were completed. Staining was done only on fibronectin, because the expression was highly seen in the compliant gels from western blot results of protein lysate. Several techniques were employed in an attempt to increase the imaged expression of fibronectin. The first technique used to visualize fibronectin was to stain the gels in their original form of the well plate. This showed that though other staining, such as in Phalloidin and DAPI was very clear, the fibronectin staining was minimal. Therefore, it was attempted to make fibronectin staining better by sectioning the gel into fragments prior to staining. This caused damage to the cells, where they were squeezed and had an altered morphology. Also, there was still very little staining seen for fibronectin. Lastly, an attempt was made in fibronectin staining by decreasing the area of the gel space, by plating in a smaller well size, 96-well plate. The fibronectin staining was not evident. These procedures did not adequately detail the presence of fibronectin within 3D encapsulated HMFs. However; there could be other techniques more successful in future experiments. Confocal microscopy is an optical imaging technique for increasing optical resolution and contrast. Also, paraffin embedding and sectioning, where thin slices are taken for more fine

staining quality, can potentially be used to view the presence of these various proteins within the gel.

Conclusions

Overall, the hypothesis was not fully proven, because ECM protein expression was not drastically different or much greater overall in the stiff gels in HMFs encapsulated than in compliant gels.. The ECM protein expression was not very conclusive in determining a strong difference of outcome between the compliant and stiff gel. Each gel type had a varied level of expression. However, several important features of the mTg gels and HMFs in mTG gels were revealed through the study. It has been shown that mTg effectively cross-links gelatin hydrogels and, at increasing concentrations, increases the mechanical stiffness of the gels. All in all, gelatin hydrogels cross-linked with 20 μ g (compliant) and 30 μ g (stiff) mTg support HMF viability and growth during the 7-day culture period. The general understanding for the study shows that HMFs are impacted by the varying environmental stiffnesses of compliant and stiff hydrogels that surrounds them during their culture when encapsulated in a 3D environment.

References

- Baek, G., Ming-Qing, G., Yoon, P. Invasive breast cancer induces laminin-332 upregulation and integrin $\beta 4$ neoexpression in myofibroblasts to confer an anoikis-resistant phenotype during tissue remodeling. *Breast Cancer Res.* 14, (2012).
- Barkan, D., Kleinman, H., Simmons, J. Tumor Cells by Targeting the Cytoskeleton Inhibition of Metastatic Outgrowth from Single Dormant. *Cancer Res.* 68, 6241-6250 (2008).
- Battista S1. The effect of matrix composition of 3D constructs on embryonic stem cell differentiation. *Biomaterials.* 2005 Nov;26(31):6194-207.
- Bott, K. The effect of matrix characteristics on fibroblast proliferation in 3D gels. *Biomaterials*, 31. 8454-8464. 2010.
- Bronzert, D., Pantazis, P., Antoniades, H. Synthesis and secretion of platelet-derived growth factor by human breast cancer cell lines. *Proceedings of the National Academy of Sciences of the United States of America*, 84, 5763–5767 (1987).
- Butcher, D.T., T. Alliston, and V.M. Weaver. A tense situation: Forcing tumour progression. *Nat. Rev. Cancer.* 9, 108–122 (2009).
- Chaffee, F. The discovery of a gravitational lens. *Sci. Am.* 243, 60-68 (1980).
- Chen CS, Mrksich M, Huang S, Whitesides GM, Ingber DE. Geometric control of cell life and death. *Science.* 276, 1425–1428 (1997).
- Chen, R., Hsiu-O, H., Ming-Thau, S. Characterization of collagen matrices crosslinked using microbial transglutaminase. *Biomaterials.* 26, 4229-4235 (2005).
- Chobert J.M., Briand L., Guegen J., Popineau Y, Larre T., Haertle T., Recent advances in enzymatic modifications of food proteins for improving their functional properties. *Nahrung*, 1996, 40, 177–182.
- Cirri, P. Cancer-associated-fibroblasts and tumour cells: a diabolic liaison driving cancer progression. *Canc Meta Rev.* 31, 195-208 (2012).
- DeSantis, M. Breast Cancer Statistics, 2011. *Ca cancer J Clin.* 61, 409–418 (2011).
- Engler, A.J., S. Sen, H.L. Sweeney, and D.E. Discher. 2006. Matrix elasticity directs stem cell lineage specification. *Cell.* 126, 677–689 (2006).
- Engler, A., Reilly, G. Intrinsic extracellular matrix properties regulate stem cell differentiation. *J. Biomech.* 43, 55–62 (2010).

Folk JE. Transglutaminases. *Ann Rev Biochem* 1980;49:517–31

Gabbiani, G. The myofibroblast in wound healing and fibrocontractive diseases. *J. Pathol.* 200, 500–503 (2003)

Gehler, S., M. Baldassarre, Y. Lad, J. Filamin A-beta1 integrin complex tunes epithelial cell response to matrix tension. *Mol. Biol. Cell.* 20, 3224–3238 (2009).

Gould V, Kouloulis G, Virtanen I. Extracellular matrix proteins and their receptors in the normal, hyperplastic and neoplastic breast. *Cell Diff Dev.* 32, 409–416.

Gudjonsson, T., Adriance, M., Sternlicht, M., Peterson, O., Bissell, M. Myoepithelial Cells: Their Origin and Function in Breast Morphogenesis and Neoplasia. *J Mam Gl Bio Neopl.* 10, 261-272 (2006).

Gupta, P. Systemic stromal effects of estrogen promote the growth of estrogen receptor-negative cancers. *Cancer Res.* 67, 2062-2071 (2007).

Hancox, R., Allen, M., Holliday, D. Tumour-associated tenascin-C isoforms promote breast cancer cell invasion and growth by matrix metalloproteinase-dependent and independent mechanisms. *Breast Cancer Res.* 2, (2009).

Hielscher AC, Qiu C, Gerecht S. Breast cancer cell-derived matrix supports vascular morphogenesis. *Am J Physiol Cell Physiol.* 302, C1243-1256 (2012).

Hinz, B., Phan, S., Thannickal, V., Galli, A., Bochaton-Piallat, M.m Gabbiani, G. The Myofibroblast: One Function, Multiple Organs. *J Amer Pathol.* 170, 1807-1816 (2007).

Ioachim, E. Immunohistochemical expression of extracellular matrix components tenascin, fibronectin, collagen type IV and laminin in breast cancer: their prognostic value and role in tumor invasion and progression. *Eur J Canc.* 38, 2362–2370 (2002).

A. Ito, A. Mase, Y. Takizawa, M. Shinkai, H. Honda, K. Hata, M. Ueda and T. Kobayashi, Transglutaminase-mediated gelatin matrices incorporating cell adhesion factors as a biomaterial for tissue engineering, *J. Biosci. Bioeng.*, 2003, 95, 2, 196–199.

Jahkola T, Toivonen T, Nordling S, von Smitten K, Virtanen I. Expression of tenascin-C in intraductal carcinoma of human breast: relationship to invasion. *Eur J Cancer.* 34, 1687-1692 (1998).

Jahkola T, Toivonen T, Virtanen I, et al. Tenascin-C expression in invasion border of early breast cancer: a predictor of local and distant recurrence. *Br J Cancer.* 78, 1507–1513 (1998).

Kalluri, R., Zeisberg, M. Fibroblasts in Cancer. *Nature Rev Cancer.* 6, 392-401 (2006).

Kim JP, Chen JD, Wilke MS, Shall TJ, Woodley DT. Human keratinocyte migration on type IV collagen. *Lab Invest.* 71, 401–408 (1994).

Kim, Sung Hoon et al. “Role of Secreted Type I Collagen Derived from Stromal Cells in Two Breast Cancer Cell Lines.” *Oncology Letters* 8.2 (2014): 507–512. *PMC*. Web. 13 June 2015.

Koochekpour S, Merzak A, Pilkington GJ. Extracellular matrix proteins inhibit proliferation, upregulate migration and induce morphological changes in human glioma cell lines. *Eur J Cancer.* 31A, 375–380 (1995).

Lo, C.M., Wang, H.B., Dembo, M., and Wang, Y.L. Cell movement is guided by the rigidity of the substrate. *Biophys. J.* 79, 144–152 (2000).

Lopez, J., Mouw, J., Weaver, V. Biomechanical regulation of cell orientation and fate. *Oncogene.* 27, 6981–6993 (2008).

Lu, P. The extracellular matrix: a dynamic niche in cancer progression. *J. Cell. Bio.* 196, 395–406 (2012).

Mangia, A. Tissue remodelling in breast cancer: human mast cell tryptase as an initiator of myofibroblast differentiation. *Histopathology* 58, 1096–1106 (2011).

Marangon, H. Laminin-5 gamma 2 chain expression is associated with intensity of tumor budding and density of stromal myofibroblasts in oral squamous cell carcinoma. *J Oral Pathol Med*, 3. 199-204. 2014.

McBeath, R., Pirone, D., Nelson, C. Cell shape, cytoskeletal tension, and RhoA regulate stem cell lineage commitment. *Dev. Cell.* 6, 483–495 (2004).

Midwood, K. The role of tenascin-C in tissue injury and tumor growth. *J. Cell Commun. Signal*, 3. 287-310. 2009.

Minz, R. Role of myofibroblasts and collagen type IV in patients of IgA nephropathy as markers of renal dysfunction. *Ind Jour Neph*, 1. 34-39. 2010.

Nakano S, Iyama K, Ogawa M. Differential tissular expression and localization of type IV collagen alpha1(IV), alpha2(IV), alpha5(IV), and alpha6(IV) chains and their mRNA in normal breast and in benign and malignant breast tumors. *Lab Invest.* 79, 281–292 (1999).

Nguyen KT, West JL. Photopolymerizable hydrogels for tissue engineering applications. *Biomaterials* 2002;23(22):4307–4314.

- Nielsen M, Christensen L, Albrechtsen R. The basement membrane component laminin in breast carcinomas and axillary lymph node metastases. *Acta Pathol Microbiol Immunol Scand.* 91, (1984).
- Nimni ME, Harkness RD. Molecular structures and functions of collagen. In: Nimni ME, editor. *Collagen*, vol. 1. Boca Raton, FL: CRC Press, 1988. p. 1–79.
- Oskarsson, T., Xiang, H., Acharyya, S. Breast cancer cells produce tenascin C as a metastatic niche component to colonize the lungs. *Nature Medicine.* 17, 867–874 (2011).
- Paszek, M., Zahir, N., Johnson, K. Tensional homeostasis and the malignant phenotype. *Cancer Cell.* 8, 241–254 (2005).
- Paguirian, A. Gelatin based microfluidic devices for cell culture. *Lab Chip.* 6, 407-413. 2006.
- Provenzano, P.P., et al., Collagen reorganization at the tumor-stromal interface facilitates local invasion. *BMC Med.* 4, (2006).
- Provenzano, P.P., et al., Collagen density promotes mammary tumor initiation and progression. *BMC Med.* 6, (2008).
- Rønnov-Jessen, L. Breast cancer by proxy: can the microenvironment be both the cause and consequence?. *Trends Mol Med.* 15, 1-13 (2009).
- Rønnov-Jessen, L., Petersen, O., Bissell, M. Cellular changes involved in conversion of normal to malignant breast: importance of the stromal reaction. *Physiol. Rev.* 76, 69–125 (1996).
- Siegel, R. Cancer Statistics, 2014. *Ca cancer J Clin.* 64, 9–29 (2014).
- Singhvi R, Kumar A, Lopez GP, Stephanopoulos GN, Wang DIC, Whitesides GM, Ingber DE. Engineering cell shape and function. *Science.* 264, 696–698 (1994).
- Sinkus, R., Lorenzen, J., Schrader, D. High-resolution tensor MR elastography for breast tumour detection. *Phys. Med. Biol.* 45, 1649–1664 (2000).
- Strutz, F., Zeisberg, M., Hemmerlein, et al. Basic fibroblast growth factor expression is increased in human renal fibrogenesis and may mediate autocrine fibroblast proliferation. *Kidney International.* 57, 1521–1538 (2000).
- Tang, N. On the equilibrium partial pressures of nitric acid and ammonia in the atmosphere. *Atmos. Environ.* 14, 819-834 (1980).

Tibbitt, M. Hydrogels as Extracellular Matrix Mimics for 3D Cell Culture. *Biotechnol Bioeng* . 103, 655–663 (2009).

Tomasek, J. Myofibroblasts and mechanoregulation of connective tissue remodeling. *Nat Rev Mol Cell Biol*. 5, 349-363. 2002.

Tsukada, T., McNutt, M., Ross, R., Gown, A. HHF35, a muscle actin-specific monoclonal antibody. II. Reactivity in normal, reactive, and neoplastic human tissues. *Am. J. Pathol*. 127, 389–402 (1987).

Pelham RJ, Jr., Wang Y. Cell locomotion and focal adhesions are regulated by substrate flexibility. *Proc Natl Acad Sci USA*1997;94:13661-13665.

William R. Harvey, Signe Nedergaard, Sodium-independent active transport of potassium in the isolated midgut of the *Cecropia* silkworm. *Proc. Natl. Acad. Sci. U.S.A.* 51, 731-735 (1964).

Williams, C., Engler, A., Slone, R. Fibronectin expression modulates mammary epithelial cell proliferation during acinar differentiation. *Cancer Res*. 68, 3182-3192 (2008).

Wozniak, M., Desai, R., Solski, P. ROCK generated contractility regulates breast epithelial cell differentiation in response to the physical properties of a three-dimensional collagen matrix. *J. Cell Biol*. 163, 583–595 (2003).

Yamashita, M. Role of stromal myofibroblasts in invasive breast cancer: stromal expression of alpha-smooth muscle actin correlates with worse clinical outcome. *Breast Cancer*. 19, 170-176 (2012).

Yu, Y., Xiao, C., Tan, L. Cancer-associated fibroblasts induce epithelial-mesenchymal transition of breast cancer cells through paracrine TGF- β signaling. *Brit. J. Canc*. 110, 724-732 (2014).

Yung, C.W. Transglutaminase crosslinked gelatin as a tissue engineering scaffold. *Wiley Per*. 83A. 1039-1046, 2007.